Submitted to Phys. Rev. A

Observation of doubly spin-forbidden rovibrational transitions in cold trapped molecular ions

A. Borodin, J. Shen and S. Schiller

Institut für Experimentalphysik,

Heinrich-Heine-Universität Düsseldorf, 40225 Düsseldorf, Germany

(Dated:)

Abstract

Rovibrational transitions in diatomic molecules whose nuclear spins, total electronic spin and rotational angular momentum are nonzero exhibit a rich hyperfine structure. The angular momentum couplings lead to selection rules that classify the rovibrational transitions into allowed, spin-forbidden and doubly-spin-forbidden transitions. Here, we demonstrate laser excitation of doubly spin-forbidden rovibrational transitions in HD^+, the most fundamental heteronuclear molecular ion having a $^2\Sigma$ ground level. The experiment is performed with molecular ions sympathetically cooled by atomic ions to a temperature of approximately 10 mK. The weak transitions are driven by a quantum cascade laser or a continuous-wave optical parametric oscillator. In the latter case, we additionally employ rotational cooling in order to increase the excitation signal, and an all-diode-laser based resonance-enhanced multiphoton dissociation (REMPD) for detection of the transition. The relevance of doubly spin-forbidden transitions for quantum state preparation of molecular ions is discussed.

I. INTRODUCTION

Weak (nearly forbidden) transitions in atoms are commonly used for precision quantum-optical experiments. For example, in the field of quantum information the atomic ground state and a long-lived metastable state can be used to encode a qubit, which is manipulated via a weak, e.g. electric quadrupole, transition connecting the two states. In optical atomic clocks, the coherent oscillation of a superposition between, e.g. a singlet $^1S_0$ and a triplet $^3P_0$ state represents the clock oscillation, and its excitation is performed by driving the spin-forbidden transition between the two states. In molecules, such transitions seem to be more rarely observed or considered in laboratory applications. Since the upper state addressed by a weak transition can also decay via allowed transitions into other states, the upper state does not usually have a very long lifetime, making detection of the weak transition more difficult.

In recent years, the field of trapped molecular ions has developed strongly. The trapping, usually in conjunction with translational cooling, allows in principle to achieve long storage time of the molecules. Then, under appropriate conditions (low collision rates, e.g. if cooling is implemented via sympathetic cooling with co-trapped atomic ions), weak transitions become accessible or detectable.

Among the molecular ions which are being studied in ion traps for spectroscopy are MgH^+ [1], AlH^+ [2], HfF^+ [3], N_2^+ [4, 5]. A species studied intensely in our group is HD^+. It possesses hyperfine structure in its full complexity: proton spin ($I_p = 1/2$), deuteron spin ($I_d = 1$), electron spin ($S_e = 1/2$) and rotational angular momentum (N). The lack of inversion symmetry is also responsible for a higher complexity of the spectra as compared to the homonuclear H_2^+. Notwithstanding its hyperfine structure, the relative simplicity of the 3-body quantum system HD^+ allows precise theoretical analysis. Its transition frequencies [6] and their strength [7] can be predicted in detail. The potential for testing quantum theory, and for fundamental physics has been described previously [8, 9]. Different transitions in

this molecular ion have already been observed [10–14]. The hyperfine structure of HD^+ has been studied extensively theoretically [7, 15] and experimentally observed and characterized [12] in two low-lying rovibrational levels. Every rovibrational level is split into 4, 10, or 12 hyperfine sub-levels, depending on whether the rotational angular momentum is $N = 0$, 1 or > 1, respectively. The splitting arises from the electron spin-proton spin interaction, the electron spin-deuteron spin interaction and the electron spin-rotational angular momentum interaction.

The existence of hyperfine structure of the rovibrational levels forces experimenters to consider ways to implement quantum state preparation, as this is helpful as a starting point for precision spectroscopy. The possibility of quantum state preparation was previously demonstrated [12], where it was also shown how this can be useful for rendering detectable transitions which normally exhibit too low a signal-to-noise ratio. The weak transition rendered detectable was a singly spin-forbidden transition, and the quantum state preparation made use of two singly spin-forbidden transitions.

Here we describe how doubly-spin-forbidden transitions are also relevant for quantum state preparation (at least in the case of HD^+), since they will eventually enable preparation of a set of molecules or a single molecule with high probability in a single, arbitrary hyperfine state. We then report the observation of two doubly spin-forbidden rovibrational transition, $(v = 0, N = 0) \rightarrow (v' = 2, N' = 1)$ at λ_s =2.65 µm, and $(v = 0, N = 2) \rightarrow (v' = 1, N' = 1)$ at λ_p =5.4 µm, respectively. The first one is an overtone electric dipole transition, which itself is weak since it becomes allowed by the small anharmonicity of the internuclear potential. In order to observe it, we developed an appropriate frequency-stabilized continuous-wave optical parametric oscillator (OPO) at 2.7 μm wavelength, which provides sufficient power. Laser rotational cooling by a commercial quantum cascade laser (QCL) is also implemented [11]. The second transition is a fundamental rovibrational transition and driven by the same QCL. A suitable system for stabilization and

tuning of the QCL frequency was developed for the purpose.

In the following, we first present the motivation for this work, then the experimental apparatus and the measurement procedures, followed by the results, and terminating with their discussion.

II. MOTIVATION

Fig. 1 (a) shows the hyperfine states' energies and states labels (approximate quantum numbers) for the ($v = 0$, $N = 0$) and ($v' = 2$, $N' = 1$) levels. The first level has four hyperfine states, while the second has 10 hyperfine states. This large number gives rise to a large number of hyperfine transitions. Fig. 2 (a) shows the relative strengths and frequencies of the various hyperfine transitions. The strongest ones are shown in red, green, blue and black. In these spin-allowed transitions, the (approximate) quantum numbers F and S do not change value, and J changes by at most one unit. Their detuning from the corresponding "spin-less" frequency $f_{0,theor}$ (the rovibrational transition frequency in absence of spin-related interactions) is comparatively small, less than ± 50 MHz, because the constants of the hyperfine Hamiltonian do not vary strongly with vibrational and rotational quantum number, see Ref. [15]. Hyperfine-state changing transitions (where at least one of F and S change value) have detunings as large as ± 1 GHz and strengths as small as 10^{-9} relative to the strongest transition. They are partially shown in pink in Fig. 2 (a). These transitions can be divided into two groups: (i) transitions in which S changes, but not F ("singly spin-forbidden"); these transitions lie inside the coloured boxes in Fig. 2 (a). Their detunings are less than ± 250 MHz and their strength is a few orders smaller than the strongest transition; (ii) Transitions in which both S and F change ("doubly spin-forbidden"). These have detunings in the range of 750 to 1000 MHz and -750 to -1000 MHz and are a few orders weaker than the singly spin-forbidden transitions. Doubly spin-forbidden transitions with

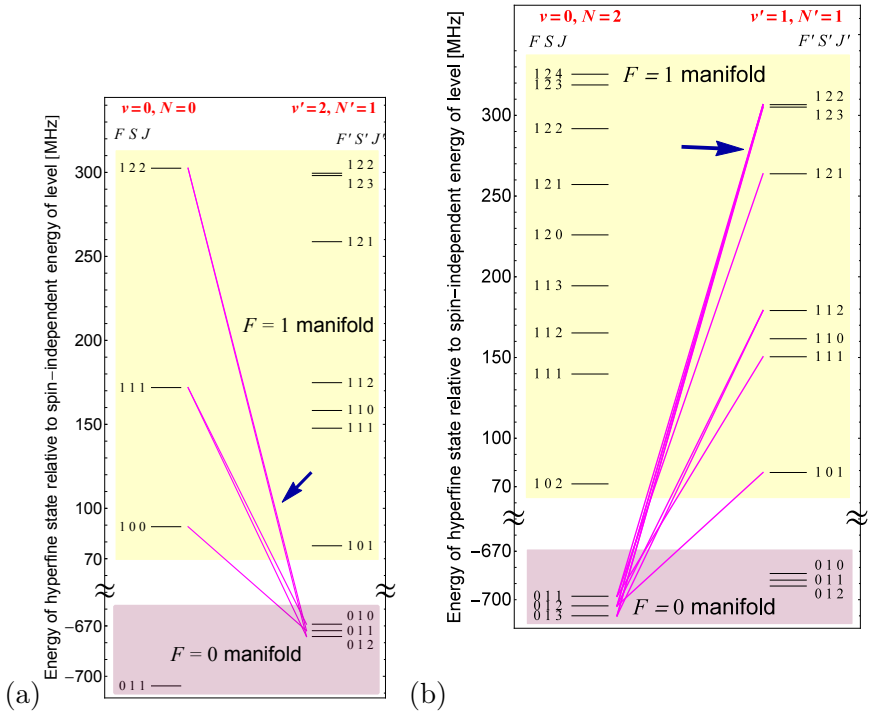

Figure 1. (Color online) Energy diagrams of the hyperfine states in the rovibrational levels relevant to the studied transitions. Inside each frame (a) and (b), on the left side are the hyperfine states of the initial rovibrational level (a) ($v = 0$, $N = 0$) and (b) ($v = 0$, $N = 2$); on the right side, are those of the final rovibrational level (a) ($v' = 2$, $N' = 1$) and (b) ($v' = 1$, $N' = 1$). The hyperfine states are labeled by the (in part approximate) quantum numbers (F, S, J). The magnetic degeneracy factor of each hyperfine state is $(2J + 1)$ (not shown). The very weak, F-manifold-changing doubly-spin-forbidden transitions (where both F and S change their values) of strength larger than 3×10^{-5} and having (a) negative frequencies or (b) positive frequencies relative to the unperturbed (spin-independent) rovibrational transition frequency $f_{0,theor}$ are shown in pink. The transitions addressed (simultaneously) by the OPO (a) or the QCL (b) used in this work are indicated by the arrows.

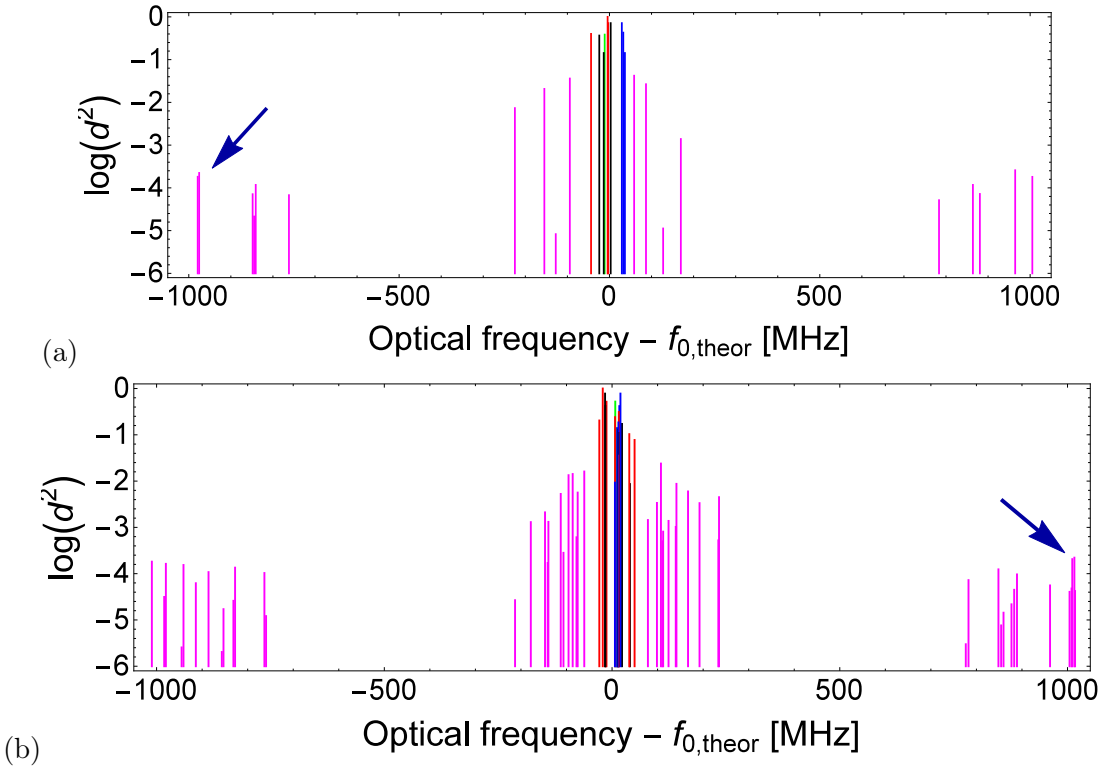

Figure 2. (Color online) Transition dipole moment squared (d^2) of the hyperfine transitions normalized to that of the strongest hyperfine transition. Zero frequency corresponds to the spin-less rovibrational transition frequency $f_{0,theor}$. (a) Hyperfine transitions for $(v = 0,\ N = 0) \rightarrow (v' = 2,\ N' = 1)$ at 2.65 µm. (b) Hyperfine transitions for $(v = 0,\ N = 2) \rightarrow (v' = 1,\ N' = 1)$ at 5.4 µm. The magnetic field is zero. In these panels, all nearly forbidden transitions are shown in pink. The two transitions dominantly addressed by the OPO or the QCL are indicated by the arrows.

negative detuning are shown in pink in Fig. 1 (a). A subset of these, namely those originating from the state $(v = 0,\ N = 0,\ F = 1,\ S = 1,\ J = 2)$ are listed in table I. The table contains also one transition in which J changes by two units, making it weaker still.

Similarly, Fig. 1 (b) shows the hyperfine states' energies for the $(v = 0,\ N = 2)$ and $(v' = 1,\ N' = 1)$ levels, and Fig. 2 (b) shows the frequencies and relative

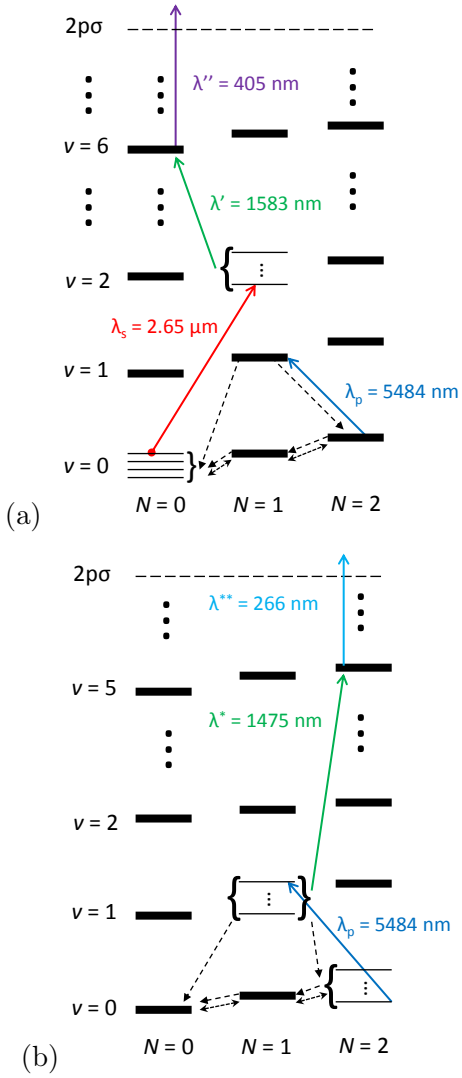

Figure 3. (Color online) Simplified energy level scheme of HD^+ with transitions relevant to this work. Full, colored arrows indicate laser-induced transitions; dashed arrows indicate spontaneous emission transitions; dotted double arrows indicate black-body-radiation-induced transitions. The doubly spin-forbidden hyperfine transitions, (a) between $(v = 0,\ N = 0)$ and $(v' = 2,\ N' = 1)$, excited by the optical parametric oscillator, is shown in red, and (b) between $(v = 0,\ N = 2)$ and $(v' = 1,\ N' = 1)$, excited by the quantum cascade laser, is shown in dark blue. Resonant laser radiations at (a) λ'= 1583 nm and (b) λ^*= 1475 nm (b) and nonresonant radiation at (a) λ''= 405 nm and (b) λ^{**}= 266 nm (b) transfer the rovibrationally excited molecular ions first to a higher vibrational level (a) $(v'' = 6, N'' = 0)$, and (b) $(v'' = 5, N'' = 2)$ and then further to electronically excited levels (predominantly $2p\sigma$), from which the ions dissociate. Rotational cooling is applied in the case (a) and occurs via optical pumping at λ= 5484 nm. The level energy differences are not to scale. The hyperfine structure is shown schematically for the levels $(v = 0,\ N = 0)$, $(v = 0,\ N = 2)$, $(v' = 1,\ N' = 1)$, and $(v' = 2,\ N' = 1)$, and as thick lines for some other levels.

strength of some of the hyperfine transitions between the corresponding states of these levels.

Let us return to the rovibrational ground level ($v = 0$, $N = 0$) of the molecule, which is the lower (initial) level for a range of possible spectroscopic studies. Counting also the Zeeman sub-states, there are altogether 12 quantum states in the ground level. From our previous work, we know that when rotational cooling by a 5.4 μm laser is performed, even the hyperfine state with the largest fractional population (the ($F = 1$, $S = 2$, $J = 2$) state) contains only approximately 20 % of all molecular ions (see also below) [12]. This is a small fraction, and it is very desirable to increase it, since this will lead to stronger signals and shorter overall measurement times. Quantum state preparation is needed for this purpose. We will now discuss that an efficient quantum state preparation requires the ability to excite doubly spin-forbidden transitions.

As a concrete example we consider the task of precision spectroscopy of the pure rotational, fundamental transition ($v = 0$, $N = 0$)$\rightarrow$($v' = 0$, $N' = 1$). This transition has already been observed [13], but not with high frequency resolution. Among its many hyperfine transitions, particularly attractive is the transition between the states ($F = 0$, $S = 1$, $J = 1$) and (F' $= 0$, S' $= 1$, J' $= 2$), since it exhibits a small Zeeman shift and a small Zeeman splitting. Its detuning from the spin-less pure rotational transition frequency $f_{0,theor}$ is $f - f_{0,theor} = -2.1$ MHz. The initial state of this transition is the energetically lowest hyperfine state of the ground level, see Fig. 1 (a). More precisely, the $J_z = 0 \rightarrow J'_z = 0$ Zeeman component exhibits a quadratic Zeeman shift approx. equal to 2.9 kHz in 1 G and whose other metrological properties have been discussed in Ref. [16]. The other two Zeeman sub-states of the lower level, $J_z = \pm 1$, can be excited to $J'_z = \pm 2$, respectively, with nearly opposite linear Zeeman shifts of approx. ∓ 40 kHz, respectively [7]. Thus, assuming a magnetic field $B = 0.035$ G, all three sub-levels of the lower hyperfine state can be excited with a 1.3 THz radiation field having

full spectral width of approx. 3 kHz. If the spectroscopy occurs in the Lamb-Dicke regime, a spectroscopic line-width of 3 kHz would be expected. At this resolution level, a precise test of the combined hyperfine energy contribution (-2.1 MHz) and a test of the QED corrections down to those of order α^5 relative to the non-relativistic transition frequency (amounting to 4 kHz [6]) would be possible.

The task of quantum state preparation would in this case be the transfer of population residing in the upper three hyperfine levels of the ground level (see Fig. 1 (a)) to the lowest-energy hyperfine level ($F = 0$, $S = 1$, $J = 1$), still in the ground state. This quantum state preparation can be implemented using a tunable laser source that drives the $(v = 0, N = 0) \rightarrow (v' = 1, N' = 1)$ transition (as using in Ref. [12]). Alternatively, the $(v = 0, N = 0) \rightarrow (v' = 2, N' = 1)$ overtone transition can be used.

However, after loading the molecular ions, and after thermalization with the black-body radiation environment, the molecular population is distributed among several rotational levels in the $(v = 0)$ manifold, only about 10 % residing in the ground level. Therefore as a first step for quantum state preparation, laser rotational cooling would be employed, as mentioned above [11, 17]. To do this, the laser which drives the transition indicated in Fig. 3 (a) as a blue line, is used to drive the most strong transitions, having near-zero detuning. This laser transfers population to the ground level $(v = 0,\ N = 0)$ via optical pumping. After optical pumping, approximately 60 % of the molecular ions will be in the ground level. Concomitantly, optical pumping also increases the population in each hyperfine state of the ground level. For example, approximately 20 % of all ions are then in the $(F = 1,\ S = 1,\ J = 2)$ hyperfine state [12].

As a second step, hyperfine pumping can be used to increase the population in a particular hyperfine state. Fig. 1 (a) shows as diagonal lines (pink) the transitions which can be used for pumping (after a number of intermediate steps) into the hyperfine state ($F = 0$, $S = 1$, $J = 1$), the lower state of the proposed spectroscopy

transition. These transitions, shown as a red and a blue arrows in Fig. 3, have the purpose of de-populating the $F = 1$ manifold of the ($v = 0$, $N = 0$) level, and the $F = 0$ manifold of the ($v = 0$, $N = 2$) level, respectively. As can be seen from Fig. 1, they include both singly and doubly spin-forbidden transitions.

More concretely, the transitions driven by the OPO, excite the ions into the rovibrational level ($v' = 2$, $N' = 1$), from which cascaded spontaneous emission to the vibrational ground levels ($v'' = 0$, $N'' = 1$) and ($v'' = 0$, $N'' = 3$) takes place. The spontaneous decays will predominantly occur on strong transitions, i.e. on spin-allowed transitions (without change in F and S). Black-body stimulated emission and spontaneous emission from these two levels to ($v''' = 0$, $N''' = 0$) and ($v''' = 0$, $N''' = 2$), respectively (short dashed lines in Fig. 3), will again leave F and S unchanged. The rotational cooling laser, when operated with near-zero detuning, will mainly induce strong transitions, and the following spontaneous decay (long dashed lines in Fig. 3) will mainly proceed on strong transitions, too. These again do not change F and S. After several cycles of these transitions, the population of the $F = 0$ state of the ground level ($v = 0$, $N = 0$) is expected to be significantly increased.

Similarly, the QCL performing the rotational cooling could be tuned to weak transitions to simultaneously provide rotational cooling and (partial) hyperfine state preparation in ($v = 0$, $N = 0$). A QCL tuned to weak transitions of ($v = 0$, $N = 1$) $\rightarrow$ (v', $N' = 0$) could perform hyperfine state preparation in ($v = 0$, $N = 1$). This is a level of interest for two-photon spectroscopy [7].

A first demonstration of hyperfine pumping, an increase of the population of the ($v = 0$, $N = 0$, $F = 1$, $S = 0$, $J = 0$) hyperfine state, which has only 5 % of total population after rotational cooling, was achieved by driving singly spin-forbidden transitions originating from ($v = 0$, $N = 0$, $F = 1$, $S = 2$, $J = 2$) and ($v = 0$, $N = 0$, $F = 1$, $S = 1$, $J = 1$) [12].

The above discussion shows that several doubly spin-forbidden transitions

(F, S, J)		Detuning, $f - f_{0,theor}$ [MHz]	Relative strength
Lower state	Upper state		
(1, 2, 2)	(0, 1, 0)	−971.5	2×10^{-7}
	(0, 1, 1)	−975.4	2×10^{-4}
	(0, 1, 2)	−978.8	2×10^{-4}

Table I. Transition strengths (relative to the strongest hyperfine transition) and precise detunings of the hyperfine transitions near -977 MHz detuning from the spin-less frequency of the $(v = 0, N = 0) \rightarrow (v' = 2, N' = 1)$ rovibrational transition. The second and third entries are the doubly spin-forbidden transitions. The first transition has $\Delta J = 2$ and is therefore extremely weak and does not contribute significantly to the detected signal.

are necessary if one needs to deplete all hyperfine states (except the goal state) and at the same time transfer the population into hyperfine states of appropriate spin structure. Below we show experimentally that such transitions can indeed be driven. In order to provide sufficient intensity for excitation of doubly spin-forbidden transitions, we developed a continuous-wave OPO, and frequency-stabilized QCL as suitable laser sources.

For the rovibrational transitions considered here, the Zeeman structure is not taken into account, because the splitting of the transition lines induced by a relatively small magnetic field (of order 1 Gauss) present in the trap, is at most a few MHz, smaller than the combined linewidth due to Doppler broadening and frequency instability of the lasers.

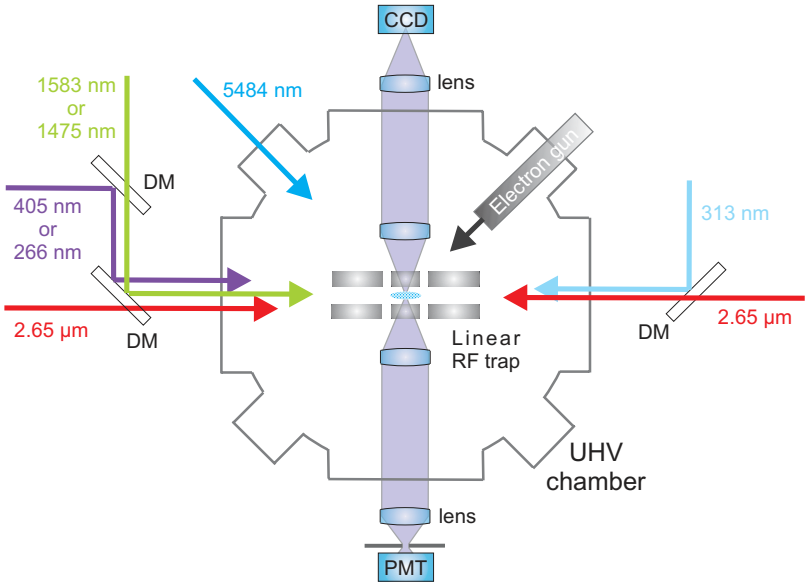

Figure 4. (Color online) Schematic of the setup and beams. DM: dichroic mirrors, CCD: charge-coupled device, PMT: photomultiplier, both are used for detection of the Be^+ fluorescence. Dimensions are not to scale.

III. EXPERIMENTAL METHOD

A. Overview

A schematic of the experimental setup is shown in Fig. 4. A linear radio-frequency quadrupole trap is operated in an ultrahigh-vacuum chamber. The trap is driven at 14.2 MHz, and is used for simultaneous trapping of Be^+ and HD^+ ions. HD^+ions are cooled sympathetically by interaction with Be^+ ions [18]. Both Be^+ and HD^+ ions are obtained from the corresponding atoms and molecules by electron impact ionization. Be atoms are generated by evaporation from metallic beryllium wire, and HD molecules are loaded into the chamber from a HD gas bottle with a piezoelectric valve.

We use a REMPD technique [19] for detection of the ions that have been vi-

brationally excited to $v' = 2$ or to $v' = 1$, see Fig. 3. In case (a), the molecules are vibrationally excited to $v' = 2$, then a 1.5 µm tunable diode laser further excites the molecules resonantly to $v'' = 6$. Then, an inexpensive, commercially available, spectrally broad 405 nm diode laser (100 mW) photodissociates the molecules from $v'' = 6$. In case (b), the molecules are first excited to $v' = 1$, and a tunable diode laser at 1.5 µm transfers the population resonantly to $v'' = 5$. For photodissociation from $v'' = 5$, we use a single-frequency 266 nm laser source (10 mW).

The laser beams involved in the REMPD excitation (1.5 µm, 405 nm, 266 nm), as well as the OPO beam (2.7 µm), are combined from the left-hand side of the setup. Laser light for cooling of Be^+ is delivered from the right-hand side. The QCL (5.4 µm) enters diagonally.

Doppler broadening arises from ion motion in the trap associated with the ion ensemble's secular temperature. We worked at the lowest secular temperature reachable, measured to be in the range 10 to 15 mK, where the corresponding Doppler broadening is approximately 5 MHz for 2.7 μm radiation (3 MHz for 5.4 μm) [12]. Micro-motion along the trap axis, at the trap RF driving frequency (here, 14.2 MHz), can contribute to the line shape of a transition.

B. The OPO

The rovibrational transition frequency of the $(v = 0,\ N = 0) \rightarrow (v = 2,\ N = 1)$ transition is $f_{0,theor} = 113.014969$ THz (2.65 µm). Among currently available continuous-wave laser sources which can generate radiation at this wavelength, OPO sources offer the highest emission power. A DFB-type diode laser with typical output power of a few mW, and previously used by us for driving a $\Delta v = 2$ transition [11] would not have been sufficient for the present purpose. We used a home-made continuous-wave, singly-resonant OPO, pumped with 9 W at 1064 nm. The resonant (signal) wavelength is 1.8 µm, and the idler wavelength is 2.65 µm.

This OPO was previously used in experiments on vibrational excitation of complex molecular ions [20], where a transition having a line-width of approx. 5 cm^{-1} was detected. In that work the OPO's wavelength was stabilized using a technique based on counter-directional mode coupling [21].

In the present work, the linewidths of transitions in HD^+, cooled to a secular temperature of 10 to 15 mK, are Doppler-limited and amount to approximately 5 MHz at 2.65 µm. In order to achieve excitation rates that are stable in time, an appropriate long-term frequency stabilization of the OPO's frequency to this level was implemented, i.e. it suppresses the frequency drift.

The first task of this stabilization is the achievement of mode-hop-free operation. To this end, a thermal lock method was used (see, e.g. [22]). Additionally, in order to stabilize the idler frequency (at 2.65 µm), its value is continuously measured and a digital feedback system based on LabView adjusts the pump laser frequency accordingly. Because no mid-IR wavemeter was available, we used a near-IR wavemeter (High Finesse Angstrom WS-7 IR). With this wavemeter, we measured alternatingly the pump (1.06 µm) and signal (1.8 µm) wavelengths c/f_{pump}, c/f_{signal}. The LabView program computed in real time the idler frequency as $f_{idler} = f_{pump} - f_{signal}$. Deviations of the idler frequency from the goal frequency $f_{0,theor} - 977\,\mathrm{MHz}$ were converted into an error signal fed back to the frequency tuning element of the pump laser.

The remaining instability of the idler frequency is illustrated by Figs. 5 a, b. As seen from the graphs, the output frequency is stabilized to within ±5 MHz relative to the goal frequency (as measured by the wavemeter). The wavemeter accuracy was checked by comparison with measurements using a frequency comb referenced to a H-maser and GPS, which provided absolute frequency accuracy. Additionally, 1.5 µm radiation from our 313 nm cooling laser source (see Ref. [23]) is used to perform a routine calibration of the wavemeter; this is possible since the 1.5 µm source is frequency-stabilized to an iodine line, providing an adequate

frequency reference. The frequency measurements by the wavemeter do not provide full information about the OPO's frequency instability since the wavemeter does not determine the OPO linewidth. We estimate the combination of frequency instability and linewidth to yield an effective full linewidth of 20 MHz.

The OPO's idler radiation is coupled into a single-mode, 3 m long ZBLAN fiber (FiberLabs Inc.) and delivered to the experimental setup. A metal-coated off-axis parabolic reflective collimator (Thorlabs, Inc.) is used to collimate the output beam. About 30 mW power is available at the output of the fiber, and after transmission through air, the power in front of the vacuum chamber window was about 10 mW. The wave is focused into the trap center, where its beam diameter is approx. 200 µm, resulting in an intensity of $I \simeq 30$ W/cm^2. The transition rate induced by this intensity is smaller than the spontaneous emission rate from the upper rovibrational level (approx. 32 s^{-1}), therefore, the relatively high power employed here (10 mW) can still be regarded as weak.

C. The quantum cascade laser (QCL)

To induce transitions between hyperfine states of ($v = 0$, $N = 2$) and ($v' = 1$, $N' = 1$), we use a QCL emitting on a single frequency at 5484 nm. When the laser performs rotational cooling, it excites the strongest (allowed) transitions [11]. For this purpose, the QCL frequency is stabilized to a reference gas absorption line. When the laser is used for excitation of a doubly spin-forbidden transition, due to the relatively large detuning from that gas' absorption line center, the laser's frequency is stabilized using a novel scheme, based on transfer cavity. A detailed description will be reported elsewhere.

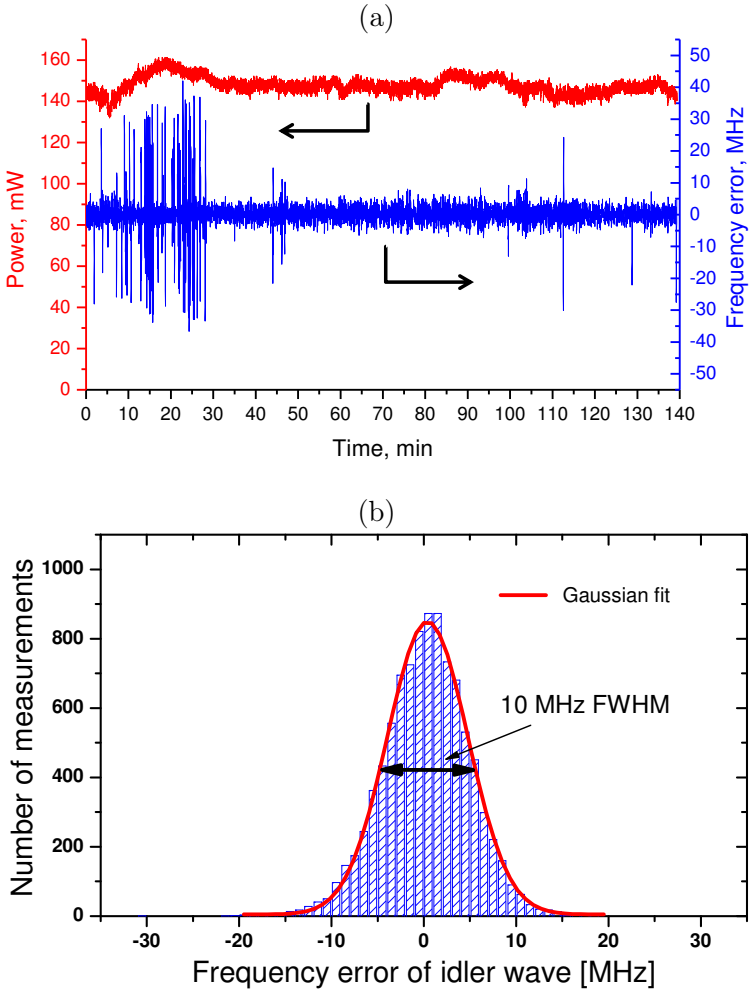

Figure 5. Frequency stabilization of the continuous-wave OPO. (a) Stability of idler frequency and output power, while the OPO is frequency-stabilized. Two data points per second are measured and plotted; (b) Histogram of the idler frequency error while the OPO is frequency-stabilized. The measurement duration was approximately 60 min.

D. Procedures

As REMPD is a destructive method, a re-loading of "fresh" HD^+ molecular ions is required after almost every cycle of measurement. Typically, reloading of Be^+ ions is not required, and the atomic ion ensemble (Coulomb cluster) can be

used during several hours of experimentation. The measurement cycle starts with loading HD^+ by opening a leak valve for introduction of HD gas and a short (1 - 3 s long) activation of the electron gun for ionization. The electron impact loading of HD^+ can produce other species, which are then also trapped and sympathetically cooled. In order to remove them from the trap, a DC potential is applied to two opposite RF electrodes of the trap, thus breaking the symmetry and reducing the quasi-potential in one of the transverse directions [24]. After loading and removal, a protocol is run which controls the lasers, secular excitation, and records signals from imaging optics and fluorescence detection. The measurement cycle is completed by removing all ions from the trap (except for the Be^+ ions) by application of appropriate secular excitation produced by an additional electrode.

We used two measurement procedures to detect the laser excitation of the doubly spin-forbidden transition. In the first procedure ("constant secular excitation"), an excitation of the transverse secular motion of the HD^+ ions is kept applied during the laser excitation of the rovibrational transition and the REMPD process. The secular excitation induces secular heating of the HD^+ molecular ion ensemble, and their energy is transferred to the Be^+ ensemble. Its increased energy is then detected as an increase in fluorescence. During REMPD, the number of HD^+ ions decreases, and consequently the Be^+ fluorescence signal decreases. This method naturally leads to a noticeable increase in the temperature of the ions, which then causes an increased Doppler broadening and is therefore not appropriate for precise transition frequency measurements.

In the second procedure ("preceding/subsequent secular excitation, p/s excitation"), the secular excitation is applied for a short time before laser excitation, then laser excitation (doubly spin-forbidden excitation and REMPD) is performed for a finite duration, followed by a second secular excitation. As in the first procedure, the fluorescence signals during the secular excitation intervals give information about the number of HD^+ ions in the trap. The normalized difference of the two

signals recorded before and after REMPD define our spectroscopic signal.

IV. RESULTS

A. OPO frequency instability test

A preliminary characterization of the excitation of the rovibrational transition was performed using approx. 10 mW and tuning it close to the spin-less transition frequency, i.e. near 0 MHz detuning from $f_{0,theor}$. The OPO then drives the strong transitions, which are shown as colored lines at the center of Fig. 2. Using the "constant excitation" method, we then observed the fluorescence signals presented in Fig. 6 (a). The ion number decreases with a rate of 0.02 s^{-1}. The relatively low rate is attributed to a limited excitation by the REMPD laser at 1.6 µm. In case (b), an additional spectral broadening of the OPO radiation by approx. ±30 MHz was applied by sweeping the pump laser frequency which in turn produces a frequency sweep of the 2.65 µm radiation.

Comparing the two cases, we find that the mean decay constant was the same, while its variance differed. The variance was approximately a factor 3 larger in case (a). We interpret this as arising from the residual frequency instability of the OPO: a moderate frequency sweep averages out the residual instability and thus reduces the fluctuations of the measurements.

B. Detection of the doubly spin-forbidden transition

In our experimental procedure, the detection of a single hyperfine transition intrinsically has a small signal-to-noise ratio (SNR). The number of HD^+ ions is low, typically a few hundred, and this population is distributed between several rotational levels. The population in the ground vibrational level is furthermore distributed over four hyperfine states, resulting in only a few ten molecules in

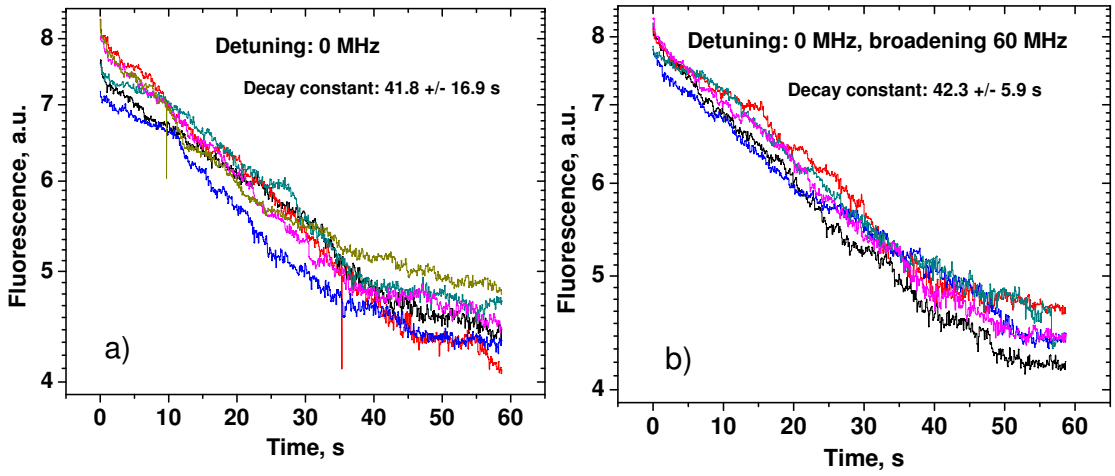

Figure 6. Excitation and detection of $(v = 0, N = 0) \rightarrow (v' = 2, N' = 1)$ transition in HD^+ molecular ions. (a) the OPO frequency was stabilized to 0 MHz detuning from $f_{0,theor}$. (b) the OPO was additionally broadened by ±30 MHz. Both cases show the same average decay constant, but the fluctuations in case (a) are larger, which is interpreted as resulting from the residual frequency instability of the OPO frequency.

the lower spectroscopy state even after rotational cooling. As a consequence, obtaining a detection with sufficient SNR requires repeating the experiment, and averaging over the obtained individual measurements. Fig. IV B(a) illustrates the excitation of the two weak doubly-spin-forbidden lines near -977 MHz detuning listed in Tab. 1, referred hereafter as "transition". Detection was made using the p/s excitation, which ensures that the HD^+ ions remain at low secular temperature, approximately 10 -15 mK. At each detuning value, we performed at least 10 measurements. The OPO+REMPD detection time was 5 seconds for each measurement. The OPO frequency was locked to the target frequency without additional broadening. The shown error bars are the standard deviation of the data.

The total time required for data acquisition of the plot of Fig. IV B (a) was about 10 hours because of the length of the individual measurement cycle that

includes molecular ion loading, cleaning, rotational cooling, transition excitation, REMPD, and ion removal.

The transition is clearly detected. It exhibits a linewidth of approximately 40 MHz, that we attribute mostly to the frequency instability of the OPO source. Note that for large enough detuning from the spin-less frequency, e.g. at -1030 MHz, almost no signal is detected. The instability of the decay values is ±5 % and represents the sensitivity of our method. It is due to the power fluctuations of the cooling laser, the variation of the number of ions in the lower spectroscopy level, and the variation in background ion loss.

According to Fig. IV B (a) the maximum fractional decay signal obtained is 10%. This is the fraction of all molecules that is dissociated via the employed transitions. Considering that the lower spectroscopy state contains approximately 20% of all ions after rotational cooling, this means that approx. 50 % of the relevant population was excited during 5 s. This is equivalent to an excitation rate of 0.14 s^{-1} . This value cannot easily be compared with a theoretical rate, due to the imperfect spatial overlap of the 2.7 μm beam focus and the molecular ions, and to the limited excitation by the REMPD laser at 1.6 µm.

Fig. IV B (b) shows the excitation of the doubly forbidden hyperfine transitions driven by the QCL and having a detuning close to 1000 MHz with respect to the spinless $(v = 0, N = 2) \rightarrow (v' = 1, N' = 1)$ transition. At least two doubly-spin forbidden transitions (detuning of 1010 MHz and 1015 MHz, respectively) with relative line strength of 2×10^{-4} each, contribute to the excitation. The linewidth of the transition, 70 MHz, is attributed to frequency instability of the QCL.

V. DISCUSSION AND CONCLUSION

We excited and observed weak, doubly spin-forbidden transitions of HD^+ in an ensemble of sympathetically cooled molecular ions. In order to achieve a sig-

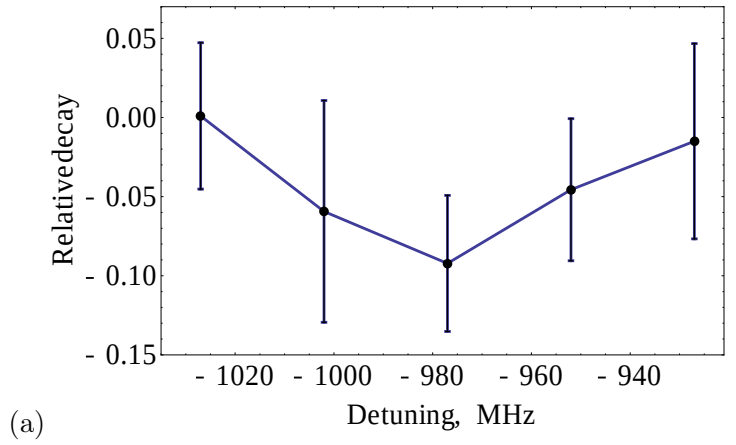

(a)

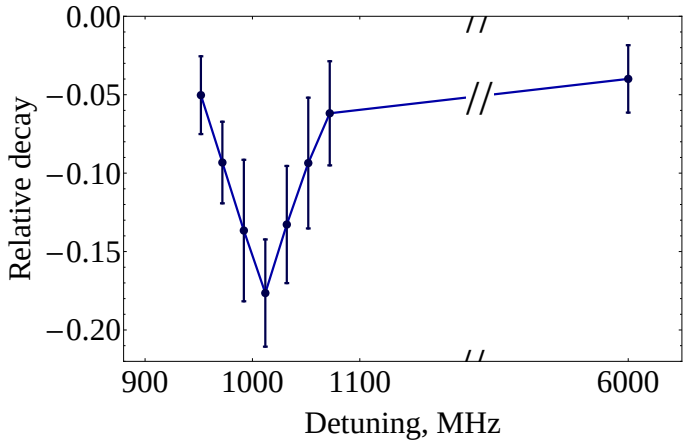

(b)

Figure 7. (a) Spectrum of a pair of doubly-spin-forbidden hyperfine transitions in the ($v = 0$, $N = 0$)→($v' = 2$, $N' = 1$) overtone transition, at a detuning near -977 MHz with respect to the spin-less transition frequency. (b) Spectrum of a pair of doubly spin-forbidden transitions in the ($v = 0$, $N = 2$)→($v' = 1$, $N' = 1$) fundamental vibrational transition, near +1010 MHz detuning.

nificant transition probability, a high-power continuous-wave optical parametric oscillator was developed. We used a destructive detection method, based on photo-dissociation of the excited molecular ions, that requires re-loading molecular ions after each experimental cycle run. The fraction of ions addressable by the studied transition determines the maximum achievable signal.

For the transition, excited by the OPO, in the ideal case of all ions initially being in the rovibrational ground level, and relative hyperfine state population according to the magnetic degeneracy, a maximum fractional ion number reduction of -0.25 would be possible. The experimentally achieved value of -0.10±0.05 means that approx. 40% of this maximum was achieved. The detected transition pair is of importance for the implementation of a "complete" quantum state preparation, which requires excitation of doubly spin-forbidden transitions to deplete all "undesired" quantum states with concomitant transfer of molecular population to an arbitrary target state. More precisely, the doubly spin-forbidden transitions are required to transfer population between the F-manifolds. In the present work, we drove two such transitions. For a full quantum state preparation into the ($F = 0$, $S = 1$, $J = 1$) hyperfine state two additional hyperfine transitions having detunings of -760 MHz and -844 MHz would have to be excited. These two transitions would be excited after appropriately frequency-tuning the OPO away from the -977 MHz transition pair to each additional frequency in turn. Our OPO system is in principle capable of doing so, as the output radiation can be tuned within approximately ±100 MHz without mode hop. Work towards implementing such a complete quantum state preparation is currently under way in our laboratory.

The transitions excited by the QCL have two initial hyperfine states of low fractional statistical population: together, it is only 0.05.

Nevertheless, in this work a signal having reasonable signal-to-noise ratio was observed. This was possible by a QCL irradiation lasting a few ten seconds. During this time, repopulation of the initial hyperfine states by black-body radiation can take place. The observed transition rate is low, and is mainly limited by this rate of re-population.

An increase of the population of the ($v = 0$, $N = 2$) initial level by optical pumping would not be straightforward because of relatively strong coupling of

this initial level by black-body radiation to the neigboring rotational levels, which does not allow for effective use of a simple rotational state preparation.

In conclusion, this work demonstrates a necessary step towards efficient hyperfine-state-selective optical pumping using doubly-forbidden transitions. We expect that such pumping will become useful for the next generation of spectroscopic studies of HD^+.

Acknowledgement: This work was done in the framework of project Schi 431/19-1 funded by the Deutsche Forschungsgemeinschaft.

---

[1] O. O. Versolato, M. Schwarz, A. K. Hansen, A. D. Gingell, A. Windberger, L. Klosowski, J. Ullrich, F. Jensen, J. R. C. Lopez-Urrutia, and M. Drewsen, Phys. Rev. Lett. **111**, 053002 (2013).

[2] C. M. Seck, E. G. Hohenstein, C.-Y. Lien, and B. C. O. P. R. Stollenwerk, arXiv:1402.0123v1.

[3] H. Loh, K. C. Cossel, M. Grau, K.-K. Ni, E. R. Meyer, J. L. Bohn, J. Ye, and E. A. Cornell, arXiv:1311.3165v1.

[4] M. Kajita, G. Gopakumar, M. Abe, M. Hada, and M. Keller, Phys. Rev. A **89**, 032509 (2014).

[5] M. Germann, X. Tong, and S. Willitsch, Nature Physics **to appear** (2014).

[6] V. I. Korobov, L. Hilico, and J. P. Karr, arXiv:1312.3728 (2013).

[7] D. Bakalov, V. Korobov, and S. Schiller, J. Phys. B: Al. Mol. Opt. Phys. **44**, 025003 (2011), corrigendum: J. Phys. B: Al. Mol. Opt. Phys., 45, 049501 (2012).

[8] B. Roth and S. Schiller, *Sympathetically cooled molecular ions: from principles to first applications, in: Cold Molecules* (R. Krems, B. Friedrich, and W. Stwalley, eds., Taylor and Francis, 2009).

[9] B. Roth, J. Koelemeij, H. Daerr, I. Ernsting, S. Jorgensen, A. W. M. Okhapkin,

A. Nevsky, and S. Schiller, Proc. in 6th Internat. Conf. In Space Optics, ESTEC, Noordwijk, The Netherlands **ESA-SP 621** (2006).

[10] J.C.J.Koelemeij, B. Roth, A. Wicht, I. Ernsting, and S. Schiller, Phys. Rev. Lett. **98**, 173002 (2007).

[11] T. Schneider, B. Roth, H. Duncker, I. Ernsting, and S. Schiller, Nature Physics **6**, 275 (2010).

[12] U. Bressel, A. Borodin, J. Shen, M. Hansen, I. Ernsting, and S. Schiller, Phys. Rev. Lett. **108**, 183003 (2012).

[13] J. Shen, A. Borodin, M. Hansen, and S. Schiller, Phys. Rev. A **85**, 032519 (2012).

[14] J. C. J. Koelemeij, D. W. E. Noom, D. de Jong, M. A. Haddad, and W. Ubachs, Appl. Phys. B **107, Issue 4**, 1075 (2012).

[15] D. Bakalov, V. I. Korobov, and S. Schiller, Phys. Rev. Lett. **97**, 243001 (2006).

[16] D. Bakalov and S. Schiller, Appl. Phys. B **114**, 213 (2014).

[17] P. Staanum, K. Hojbjerre, P. Skyt, A. Hansen, and M. Drewsen, Nature Physics **6**, 271 (2010).

[18] P. Blythe, B. Roth, U. Frohlich, H. Wenz, and S. Schiller, Phys. Rev. Lett. **95**, 183002 (2005).

[19] B. Roth, J. C. J. Koelemeij, H. Daerr, and S. Schiller, Phys. Rev. A **74**, 040501 (2006).

[20] C. Wellers, A. Borodin, S. Vasilyev, D. Offenberg, and S. Schiller, Phys. Chem. Chem. Phys. **13**, 18799 (2011).

[21] S. Vasilyev, H. Gollnick, A. Nevsky, A. Grisard, E. Lallier, J. J. B. Gerard, and S. Schiller, Appl. Phys. B **100**, 737 (2010).

[22] M. Vainio, J. Peltola, S. Persijn, F. Harren, and L. Halonen, Appl. Phys. B **94**, 411 (2009).

[23] S. Vasilyev, A. Nevsky, I. Ernsting, M. Hansen, J. Shen, and S. Schiller, Appl. Phys. B **103**, 27 (2011).

[24] U. Froehlich, B. Roth, and S. Schiller, Physics of Plasma **12**, 073506 (2005).